Contents lists available at ScienceDirect

Stem Cell Research

journal homepage: www.elsevier.com/locate/scr

Ocular surface ectoderm instigated by WNT inhibition and BMP4

Yuki Kobayashi[a,b], Ryuhei Hayashi[a,b,*], Shun Shibata[b,c], Andrew J. Quantock[d], Kohji Nishida[a,e]

[a] Department of Ophthalmology, Osaka University Graduate School of Medicine, 2-2 Yamadaoka, Suita, Osaka 565-0871, Japan
[b] Department of Stem Cells and Applied Medicine, Osaka University Graduate School of Medicine, 2-2 Yamadaoka, Suita, Osaka 565-0871, Japan
[c] Research and Development Division, ROHTO Pharmaceutical Co Ltd, Osaka, Osaka 544-8666, Japan
[d] Structural Biophysics Group, School of Optometry and Vision Sciences, College of Biomedical and Life Sciences, Cardiff University, Cardiff, CF24 4HQ Wales, UK
[e] Integrated Frontier Research for Medical Science Division, Institute for Open and Transdisciplinary Research Initiatives (OTRI), Osaka University, Suita, Osaka 565-0871, Japan

ARTICLE INFO

ABSTRACT

We sought to elucidate how and when the ocular surface ectoderm commits to its differentiation into the corneal epithelium in eye development from human induced pluripotent stem cells (hiPSCs) under the influence of WNT signaling and the actions of BMP4. These signals are key drivers ocular surface ectodermal cell fate determination. It was discovered that secreted frizzled related protein-2 (SFRP2) and Dickkopf1 (DKK1), which are expressed in neural ectoderm, are both influential in the differentiation of hiPSCs, where they act as canonical WNT antagonists. BMP4, moreover, was found to simultaneously initiate non-neural ectodermal differentiation into a corneal epithelial lineage. Combined treatment of hiPSCs with exogenous BMP4 aligned to WNT inhibition for the initial four days of differentiation increased the ocular surface ectodermal cell population and induced a corneal epithelial phenotype. Specification of a surface ectodermal lineage and its fate is thus determined by a fine balance of BMP4 exposure and WNT inhibition in the very earliest stages of human eye development.

1. Introduction

The cornea is the transparent, anterior portion of the eye via which light enters and is focused towards the retina. The corneal epithelium, a cellular multi-layer that shrouds the cornea's outer surface, undergoes constant cell renewal throughout life and is essential for healthy vision. The corneal epithelium develops from the ocular surface ectoderm via a mechanism in which the transcription factor deltaNp63 (p63) is instrumental. A well-established ectodermal progenitor marker which helps determine embryonic epidermal fate and epithelial homeostasis (Aberdam et al., 2007; Melino et al., 2015; Senoo et al., 2007; Soares and Zhou, 2018; Yoh and Prywes, 2015), p63 is abundantly expressed in the basal layers of the corneal epithelium at the limbus (the area at the edge of the cornea where corneal stem cells reside) and epidermis. Another ocular surface ectodermal marker, which plays a pivotal role in regulating optic cup patterning and eye development is paired box 6 (PAX6) (Shaham et al., 2012), and both p63 and PAX6 genes are co-expressed in the corneal epithelium, acting as critical indicators of corneal epithelial lineage.

Recently, we described the generation on a laminin 511 substrate of a two-dimensional colony of hiPSC-derived cells, termed a SEAM (a self-formed ectodermal autonomous multi-zone) in which cells formed four distinct concentric zones (Hayashi et al., 2016; Shibata et al., 2018). In each zone, cells exhibited characteristics of different tissues of the developing eye; lens, retina cornea, for example. We further devised a method to isolate and obtain presumptive SEAM-derived corneal epithelial cells with a cultivation period of 10–12 weeks (Hayashi et al., 2017).

The current study was conducted to interrogate the mechanisms of ocular surface ectodermal development using a newly generated p63-EGFP knock-in hiPSC reporter line (Kobayashi et al., 2017). Ocular surface ectodermal cells that co-expressed both p63 and PAX6 already existed in the SEAMs after only 10 days in culture. Here, we show that inhibition of the WNT signaling pathway and the simultaneous action of endogenous Bone Morphogenetic Protein 4 (BMP4) in the very earliest stages of hiPSC differentiation positively influence p63 and PAX6 expression, and are thus essential drivers for the induction of ocular surface ectoderm and its differentiation into corneal epithelium.

2. Material and methods

2.1. Cell line and culture conditions

Generation of the p63-EGFP knock-in hiPSC reporter line was described previously (Kobayashi et al., 2017). It was derived from a human iPSC line, 1383D2, which was used as an experimental control (WT, wildtype). Cells were cultured in StemFit medium (Ajinomoto, Tokyo, Japan) on dishes coated with laminin-511E8 (iMatrix-511, nippi, Tokyo, Japan). Cells were passaged every seven days, changing the medium every two days (Nakagawa et al., 2014). All experimental procedures using recombinant DNA were approved by the Recombinant DNA Committee of Osaka University.

2.2. Differentiation of hiPSCs into ocular ectodermal cells

p63-EGFP knock-in hiPSCs were induced to differentiate into ocular-like ectodermal cells as part of a SEAM as described in detail elsewhere (Hayashi et al., 2017, 2016). Briefly, cells were seeded in dishes pre-coated with laminin-511E8, and grown in StemFit medium for 8–12 days. To induce ocular differentiation, the StemFit medium was replaced with differentiation medium (DM) based on Glasgow-MEM (Thermo Fisher Scientific) supplemented with 10% Knockout Serum Replacement (Thermo Fisher Scientific), 1 mM sodium pyruvate (Thermo Fisher Scientific), 0.1 mM non-essential amino acids (Thermo Fisher Scientific), 2 mM L-glutamine (Thermo Fisher Scientific), 1% penicillin–streptomycin, and 55 μM monothioglycerol (Wako, Osaka, Japan). After four weeks, cells were cultured for another four weeks in corneal differentiation medium (CDM; diluted 1:1 in DM and Cnt-PR (without EGF and FGF2)) (CELLnTEC Advanced Cell Systems, Bern, Switzerland) supplemented with 20 ng/mL KGF (Wako), 10 μM Y-27632 (Wako) and 1% penicillin–streptomycin. Cells were treated with the respective compounds; BMP4 (1 ng/mL, R&D systems, MN, USA), IWP2 (1 μM, Wako), CHIR99021 (10 μM, Wako), LDN193189 (10 nM, Wako), retinoic acid (1 μM, Sigma-Aldrich, St. Louis, MO), SB431542 (10 μM, Wako), rhTGFB2 (10 ng/mL, Wako), JNK-IN-8 (10 μM, Selleck chemicals, Houston, TX) from day 0 to 4. Cells were treated with the respective compounds; BMP4 (1 ng/mL), IWP2 (1 μM, Wako) from day 4 to 7. After treatment the medium was changed to DM without the compounds. Cells treated with DMSO was used as an experimental control.

2.3. Flow cytometry and cell sorting

p63-EGFP knock-in hiPSCs were differentiated for 10 days or 6 weeks, dissociated with Accutase (Thermo Fisher Scientific) for 60–90 min at 37 °C, harvested through a 40 μm cell strainer (BD Biosciences, San Diego, CA), and collected into keratinocyte culture medium (KCM; a 3:1 mix of DMEM without glutamine and Nutrient Mixture F-12 Ham; Thermo Fisher Scientific) supplemented with 5% fetal bovine serum (Japan Bio Serum, Hiroshima, Japan), 0.4 μg/mL hydrocortisone succinate (Wako), 2 nM 3,3′,5-triiodo-l-thyronine sodium salt (MP Biomedicals, Santa Ana, CA), 1 nM cholera toxin (List Biological Laboratory, Campbell, CA), 2.25 μg/mL bovine transferrin HOLO form (Thermo Fisher Scientific), 2 mM L-glutamine, 0.5% insulin transferrin selenium (Thermo Fisher Scientific), and 1% penicillin–-streptomycin. Cells were washed in phosphate-buffered saline. The 1383D2 cell line was used as an EGFP (enhanced green fluorescent protein) negative control. Cells were sorted on a SH800 Cell Sorter (Sony Biotechnology Inc., Tokyo, Japan) and the data were analyzed using SH800 software.

2.4. Cytospin experiments

For immunofluorescence staining, sorted cells were adjusted to a density of 5–8 × 10^5 cells/mL, and 200 μL of the cell suspension was centrifuged at 1000 rpm for 5 min in a Cytospin™ 4 Cytocentrifuge (Thermo Fisher Scientific). Cells were stained according to the method for immunofluorescence staining and were counterstained with Hoechst 33342 (Thermo Fisher Scientific) to visualize the nuclei before being imaged by fluorescence microscopy (Axio Observer. Z1, Carl Zeiss, Jena, Germany). At least 100 cells were counted in three to six different images for each experiment, and quantified the ratio of p63 + /PAX6 + cells.

2.5. Immunofluorescence staining

Mouse embryonic tissue sections were fixed for 20 min at room temperature in cold methanol, after which they were washed with Tris-buffered saline (TBS, Takara Bio, Otsu, Japan) three times for 10 min each. Cells on slides after cytospin or on 12-well plate were fixed for 20 min at room temperature in 4% paraformaldehyde and similarly washed. Samples were incubated for 1 h in Tris-buffered saline containing 5% donkey serum (Jackson ImmunoResearch Laboratories, Inc., West Grove, PA) and 0.3% Triton X-100 (Wako). They were then probed overnight at 4 °C with antibodies against p63 (4A4; Santa Cruz Biotechnology, Santa Cruz, CA) and PAX6 (PRB-278P; Covance Research Products, Denver, PA) in TBS containing 1% donkey serum and 0.3% Triton X-100. Subsequently, samples were labeled for 1 h at room temperature with secondary antibodies conjugated to Alexa Flour 488 and 568 (Thermo Fisher Scientific). Cells were counterstained with Hoechst 33342 (Thermo Fisher Scientific) to visualize the nuclei, and imaged by fluorescence microscopy (Axio Observer. Z1, Carl Zeiss, Jena, Germany).

2.6. qRT-PCR experiments

Differentiated hiPSCs were harvested at specific timepoints and lysed in QIAzol reagent (Qiagen, Venlo, Netherlands). Total RNA was extracted and reverse-transcription was performed using the SuperScript III First-Strand Synthesis System for qRT-PCR (Thermo Fisher Scientific). Synthesized cDNA was amplified in duplicate on an ABI Prism 7500 Fast Sequence Detection System (Thermo Fisher Scientific) using TaqMan Fast Universal PCR Master Mix (Applied Biosystems). Targets were amplified with TaqMan MGB probes assays against TaqMan probes (Table S1). Thermocycling conditions for the TaqMan reactions consisted of an initial cycle at 95 °C for 20 s, followed by 45 cycles at 95 °C for 3 s and 60 °C for 30 s.

2.7. ELISA analysis

SFRP2 and DKK1 were quantified in cell culture supernatants. The initial seeding density was 6000 cells per six-well plate. The supernatant at day 0 was collected at the start of differentiation (i.e. after 10 days of hiPSC culture in StemFit), whereas the supernatants at day 3 were collected after 3 days of differentiation medium (DM) culture. StemFit and DM were used for internal control, respectively. The samples were reacted in duplicate or triplicate in a 96-well plate using the human SFRP2 ELISA kit (Cloud-Clone Corp., Katy, TX) and human DKK1 ELISA kit (R&D systems) according to the manufacturer's instructions. The activity was measured in a multilabel counter (ARVO MX, Perkin Elmer, Waltham, MA).

2.8. Blocking assay

p63-EGFP knock-in hiPSCs were incubated with SFRP2 (80.8.6; Millipore, MA, USA), DKK1 (R&D systems) or mouse IgG2a, kappa monoclonal (MOPC-173; abcam, Cambridge, U.K), goat IgG polyclonal (abcam) from 0 to 3 days of differentiation. Cells were analyzed by FACS and cytospin at 10 days of differentiation. All final concentrations were adjusted to 100 μg/mL.

(caption on next page)
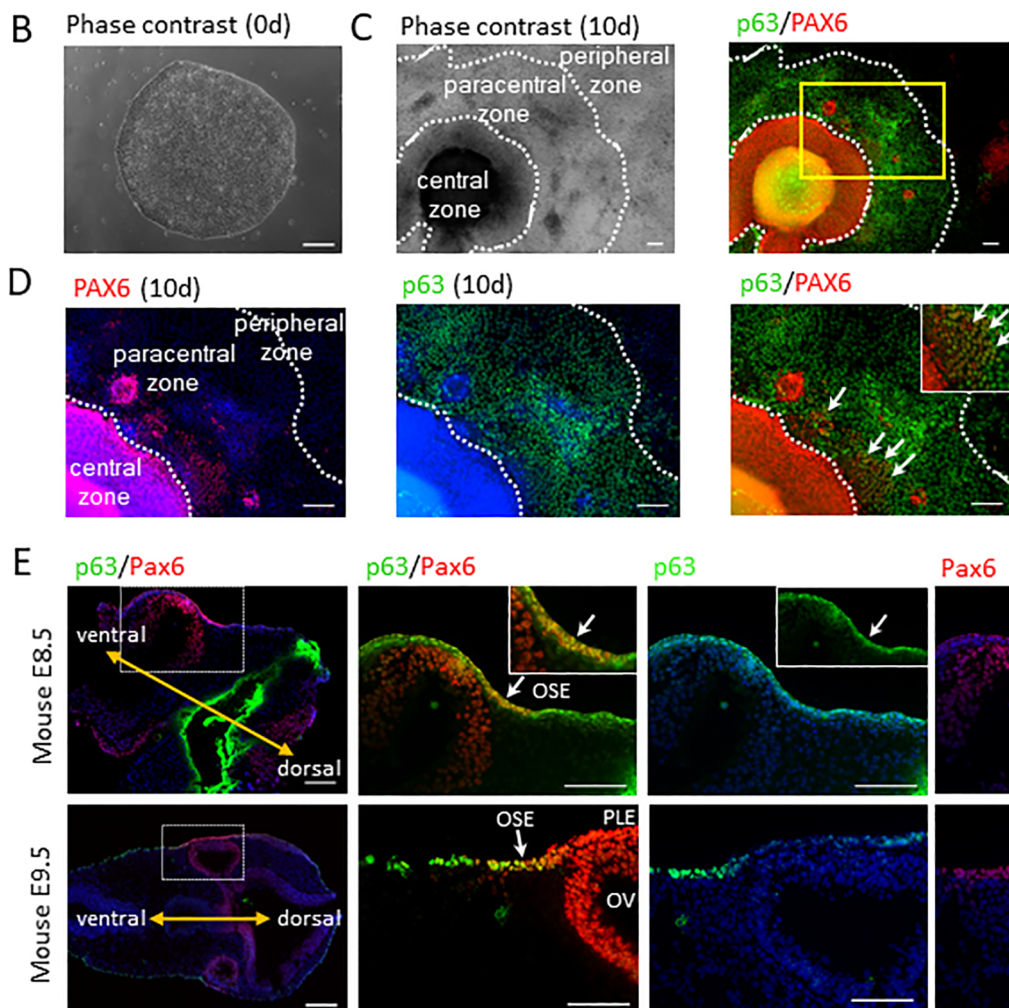
Fig. 1. Schematic description of ocular surface lineage epithelial development and differentiation of p63-EGFP knock-in hiPSCs into early ocular surface ectoderm. (A) Schematic description of ocular surface ectodermal development in an embryonic eye and a pre-SEAM structure of differentiated human iPSCs at 10 days and a SEAM structure at 6 weeks of differentiation. The cell culture duration, mediums, cell treatments and analysis time points are shown. The cells were treated 1) from 0 to 4 days with BMP4, LDN 193189 (LDN), TGFβ, SB431542 (SB), retinoic acid (RA), JNK-IN-8 (JI8), IWP2, IWP2 + BMP4 (I + B), IWP2 + LDN (I + L), CHIR99021 (CHIR), CHIR + BMP4 (C + B), and CHIR + LDN (C + L), or 2) from 4 to 7 days with BMP4, IWP2, or I + B. CE, corneal epithelium; CDM, Corneal Differentiation Medium; DM, Differentiation Medium; EK, epidermal keratinocyte; CNS, central nervous system; NR, neuroretina; OSE, ocular surface ectoderm; SE, surface ectoderm; LE, lens; NC, neural crest; OC, optic cup; RPE, retinal pigment epithelium; NE, neural ectoderm. (B) A representative phase contrast image of a colony of undifferentiated hiPSCs at 0 day (scale bar, 200 μm). (C) Characterization of differentiated p63-EGFP knock-in hiPSCs into ocular cells in the pre-SEAM structure at 10 days of differentiation (scale bar, 100 μm). Immunofluorescence staining for ocular cells markers; p63 expression (green) was detected in the paracentral zone and PAX6 expression (red) was detected in the central and paracentral zone. Nuclei, blue. (D) Higher magnification images of highlighted zone from C. The white arrows indicate p63 + /PAX6 + cells in the paracentral zone (scale bar, 100 μm). (E) p63 + /Pax6 + cells in mouse embryonic eyes at E8.5 and E9.5 (left panels; upper and bottom, scale bar, 200 μm and the other pictures, scale bar, 100 μm). p63 (green) and Pax6 (red) in the embryos. Nuclei, blue. The white arrows indicate p63 + /Pax6 + cells. The yellow allows indicate ventral and dorsal. OSE, ocular surface ectoderm; PLE, presumptive lens ectoderm; OV, optic vesicle.

2.9. Statistical analysis

Data are represented as the mean ± standard error for each group. n represents technical replicates. Statistical significance was analyzed via Wilcoxon rank sum test, steel test, and Steel–Dwass test using JMP ver. 14.0.0 software (SAS institute Japan Co. Ltd., Tokyo, Japan). All statistical analyzes were conducted with a significance level of α = 0.05 (P < 0.05).

3. Results

3.1. Ocular surface ectoderm expresses p63 and PAX6, and is located in a paracentral zone at 10 days of differentiation and mouse embryonic eyes

After 6 weeks of differentiation following our previously reported protocols (Hayashi et al., 2017, 2016), characteristic 4-zone SEAMs could be formed (Fig. 1A). Earlier in the cultivation period, however, (i.e. after 10 days of differentiation) p63-EGFP knock-in hiPSCs were found to have generated an immature pre-SEAM with three zones; central, paracentral, and peripheral (Fig. 1C, phase contrast), which emerge from initial colonies of undifferentiated cells (Fig. 1B). Ocular surface ectoderm that express p63 and PAX6 was confined to the paracentral zone of the 10-day pre-SEAM as identified by immunofluorescence staining (Fig. 1C), and these were invariably located close to its inner boundary with the central zone as indicated by white arrows in Fig. 1D. On the other hand, cells in the central zone were p63 negative and PAX6 positive due to a neuroectodemal cell fate. In mouse embryonic eyes at E8.5 and E9.5, p63 + /Pax6 + cells were localized within an area of ocular surface ectoderm. In contrast, the presumptive lens ectoderm with p63 negative cells at E9.5 was located between the ocular surface ectoderm with its p63 + /Pax6 + cells (Fig. 1E).

3.2. Exogenous BMP4 enhances p63 expression in immature pre-SEAMs and mature SEAMs in conjunction with WNT inhibition

To establish the molecular mechanisms that underpin surface ectodermal commitment, we treated p63-EGFP knock-in hiPSCs with small molecules and/or growth factors to activate and/or inhibit key signals involved in eye development. After treatment for the initial 4 days of differentiation in DM (Fig. 1A) p63-enhanced green fluorescent protein positive (p63-EGFP +) cells were quantified by FACS in the immature 3-zone pre-SEAM (at 10 days of differentiation) and the mature 4-zone SEAM (at 6 weeks of differentiation) (Fig. 2A–D). BMP4 and TGFβ influence epithelial development (Hayashi et al., 2016), and here we show that cells treated with a BMP4 inhibitor (LDN193189 (LDN)) or a TGFβ inhibitor (SB431542 (SB)) failed to express p63 either at 10 days or 6 weeks of differentiation. We also discovered that exogenous BMP4 increased the number of p63 + cells (1.02-fold at 10 days of differentiation and 1.48-fold at 6 weeks of differentiation) compared to DMSO controls, whereas additional TGFβ did not elevate p63 expression (Fig. 2C and D).

Previous studies have suggested a link between BMP4 and the WNT signaling pathway in the induction of surface ectoderm during development (Patthey et al., 2009), and there are reports of WNT signaling inhibition disturbing eye development (Fujimura, 2016; Sugiyama et al., 2013). To determine how WNT signaling contributes to ocular surface ectodermal commitment, cells were treated with WNT inhibitors or a WNT activator. Treatment with WNT signaling inhibitor IWP2 reveals that p63-EGFP + cells show 1.2-fold increase at 10 days of differentiation, and at 6 weeks of differentiation levels show 4.3-fold increase. IWP2 in combination with BMP4 (Fig. 2 (I + B)) shows 1.5-fold increase p63 at 10 days of differentiation and 5.1-fold increase p63 at 6 weeks of differentiation. IWP2 plus LDN (Fig. 2 (I + L)), on the other hand, decreases p63 + cells as expected (0.2-fold at 10 days of differentiation and 0.49-fold at 6 weeks of differentiation) due to the suppression of BMP4 signaling (Fig. 2C and D). WNT inhibition, therefore, is not sufficient to promote the differentiation of hiPSCs into ocular surface ectoderm in and of itself; BMP4 signaling is required too.

IWP2 acts to block both canonical and non-canonical WNT signaling pathways owing to the inhibition of WNT secretion and processing. More specifically, the kinase JNK is involved in the non-canonical pathway via the activation of cJUN. To examine if JNK signaling and the non-canonical pathway are involved in surface ectodermal differentiation into a corneal epithelial lineage and p63 expression, we used a specific JNK signaling inhibitor (JNK-IN-8 (JI8)) to treat p63-EGFP knock-in hiPSCs for 4 days at the start of DM cultivation (Fig. 1A). The results showed that JI8-treated cells abundantly expressed p63 after both 10 days and 6 weeks of differentiation. WNT signaling activation by GSK inhibitor CHIR99021 (CHIR) during the initial 4 days of differentiation completely blocked p63, an outcome that was not mitigated by the addition of exogenous BMP4 along with CHIR (Fig. 2 (C + B)). Likewise, LDN and CHIR in combination (Fig. 2 (C + L)) did not stimulate p63 expression as expected. SEAM formation was grossly abnormal, with no distinctive zonal formation, when p63-EGFP knock-in hiPSCs had been treated with CHIR from days 0–4, and this was the case when BMP4 or LDN had been used too. At 6 weeks of differentiation, p63 was expressed in CHIR treated cells, with and without BMP4 or LDN, but not in cells at 10 days of differentiation.

To ascertain at what stage in the differentiation process the induction of ocular surface ectoderm from ectoderm was initiated we treated cells with IWP2 and/or BMP4, (i) from 0 to 4 days of differentiation and (ii) from 4 to 7 days of differentiation (Fig. 1A). This revealed that early (i.e. day 0–4) IWP2 and IWP2/BMP4 treatment resulted in a significantly higher differentiation efficiency of p63 + /PAX6 + in EGFP + cells than later (i.e. day 4–7) treatment (Fig. S1), signifying that epithelial induction occurs early in surface ectoderm differentiation.

3.3. Retinoic acid enhances p63 expression in hiPSCs at 10 days, but not at 6 weeks

Retinoic acid (RA) is an essential factor in eye development (Matt et al., 2005). To investigate the role RA signaling in the development of the ocular surface ectoderm, p63-EGFP knock-in hiPSCs were treated with additional RA for the initial 4 days of differentiation in DM
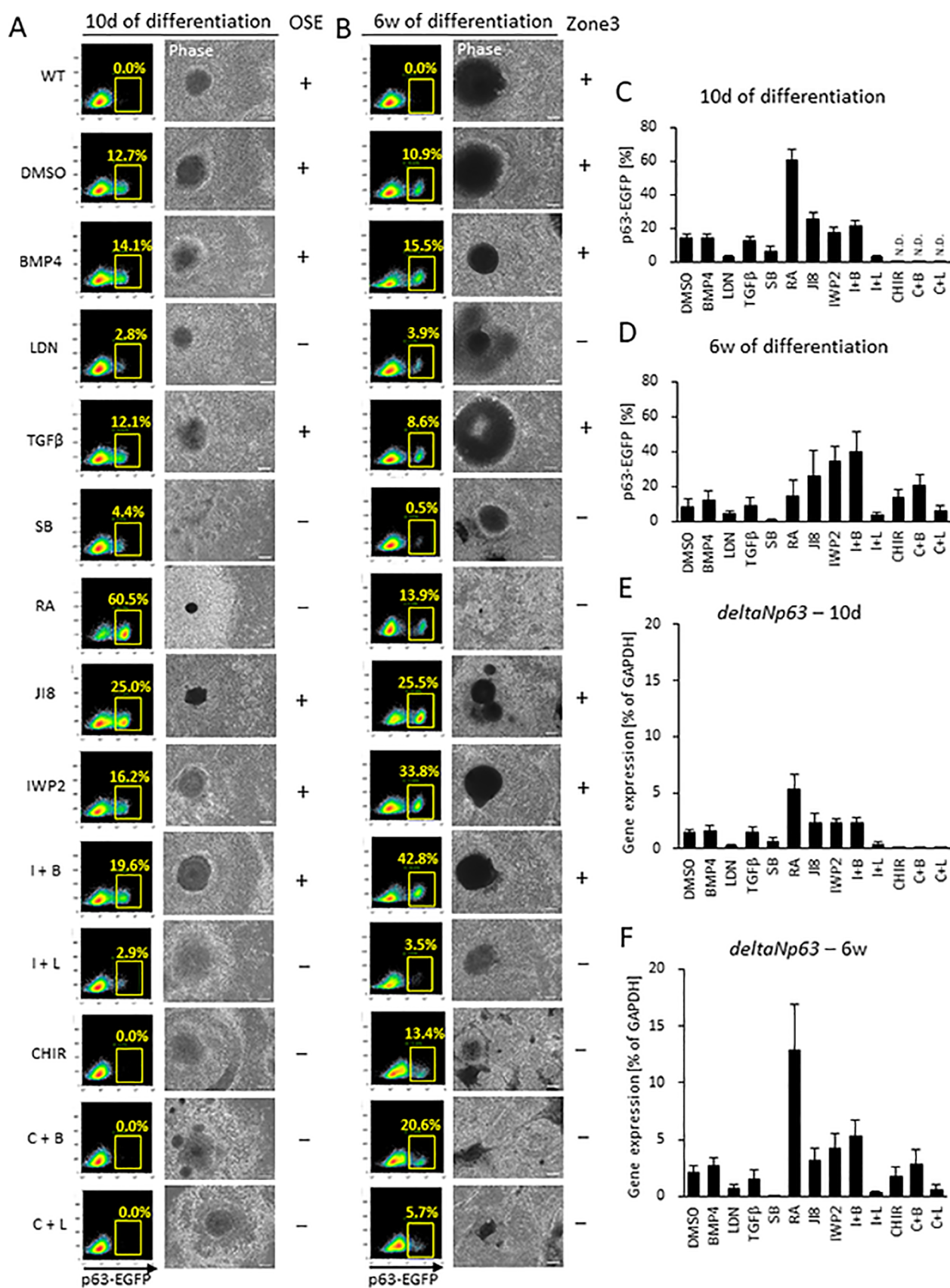
(caption on next page)

Fig. 2. **Expression of p63 in surface ectodermal cells differentiated from p63-EGFP knock-in hiPSCs.** (A, B) Fluorescence-activated cell sorting (FACS) based on p63 expression at 10 days and 6 weeks of differentiation. The cells were treated from 0 to 4 days with BMP4, LDN, TGFβ, SB, RA, JI8, IWP2, IWP2 + BMP4 (I + B), IWP2 + LDN (I + L), CHIR, CHIR + BMP4 (C + B), and CHIR + LDN (C + L). Wild-type (WT) is a negative control for FITC signal. The plots are representative of samples at 10 days and 6 weeks of differentiation, respectively. The percentage of EGFP in plots indicates an average value. Representative phase contrast images are at 10 days and 6 weeks of differentiation (scale bar, 100 μm). Observation of ocular surface ectoderm (OSE) at 10 days of differentiation and of SEAM zone 3 at 6 weeks of differentiation are indicated by a plus (+); an absence is noted by a minus (−). (C, D) The average ratio of p63-EGFP population [%] in 10 days and 6 weeks of differentiated cells. (E, F) Gene expression levels of p63 correlated to EGFP positive cells. Data shown as the mean ± SD (n = nine independent experiments for DMSO, BMP4, IWP2, and I + B, n = six independent experiments for LDN, RA, I + L, CHIR, C + B, and C + L, n = seven independent experiments for TGFβ, and SB, n = five independent experiments for JI8 at 10 days of differentiation, n = eight independent experiments for DMSO, BMP4, IWP2, and I + B, n = five independent experiments for LDN, TGFβ, SB, RA, JI8, I + L, CHIR, C + B, and C + L at 6 weeks of differentiation). N.D. Not determined.

(Fig. 1A). As seen from the average ratios of p63-EGFP+ cells at 10 days and 6 weeks of differentiation (Fig. 2C and D), RA treatment dramatically increased p63-EGFP+ cells at 10 days, but not 6 weeks, of differentiation. Quantitative real-time reverse-transcriptase PCR (qRT-PCR) results confirmed that *p63* expression correlated with the prevalence of p63-EGFP+ cells at these time points (Fig. 2E and F). An evaluation of the morphology of ocular surface ectodermal-like cells in the immature pre-SEAM and the mature SEAM revealed that if ocular surface ectodermal-like cells had not developed in the pre-SEAM by 10 days of differentiation, then without exception they did not form in zone 3 of the mature SEAM at 6 weeks of differentiation (Fig. 2A and B).

3.4. Promoting the induction of ocular surface ectoderm by the inhibition of WNT signaling and exogenous BMP4 signaling

To assess the proportion of ocular surface ectodermal cells that express both p63 and PAX6, we isolated p63-EGFP+ cells at 10 days and 6 weeks of differentiation and quantified the p63+/PAX6+ cell ratio based on immunostaining characteristics (Fig. 3A and B). This analysis was not conducted for cells treated with CHIR, CHIR + BMP4, and CHIR + LDN at 10 days of differentiation, and with SB at 6 weeks of differentiation because of the previously ascertained negative expression of p63-EGFP+ cells (Fig. 2C and D). The differentiation efficiency of p63+/PAX6+ cells was determined by assessing the total cell number, the percentage of p63-EGFP+ cells (ascertained by FACS analysis), and the PAX6+ cell ratio in EGFP+ cells obtained by the cytospin method (Fig. 3C, Fig. S3A and S3B). This analysis revealed that cells treated with IWP2 and/or exogenous BMP4 signaling have a significantly enhanced p63+/PAX6+ differentiation efficiency at 10 days of differentiation, which was further increased by 6 weeks of differentiation. By immunofluorescent staining, zone 3 with its p63+/PAX6+ cells, was larger following IWP2 and BMP4 treatment compared with non-treated DMSO controls (Fig. 3D).

### 3.5. Canonical and non-canonical WNT signaling during early differentiation

To discern the treatment efficiency of the various small molecules during the initial 4 days of differentiation we examined gene expression patterns for the WNT (Fig. 4A) and BMP4 signaling pathways (Fig. 4B) at the end of this period, and confirmed that canonical WNT signaling genes (*WNT1* and *WNT3A*) were significantly downregulated in IWP2-treated cells (i.e. IWP2 and I + B) compared to DMSO controls. Canonical WNT activation was confirmed by the discovery that canonical WNT target genes such as *AXIN2* and *LEF1* were elevated in CHIR-treated cells. WNT inactivation in IWP2-treated cells was confirmed by the suppression of *AXIN2* and *LEF1*. Additionally, non-canonical WNT signaling genes (*WNT5A* and *WNT11*) were upregulated in CHIR-treated cells. We also treated cells with JI8 to reduce the levels of JNK downstream genes such as cJUN. This showed that *cJUN* gene expression was considerably reduced by JNK inhibition (Fig. 4A). These results indicate that IWP2 is effective in inhibiting the canonical WNT pathway, and CHIR is effective in activating both canonical and non-canonical WNT pathways. Our experiments also revealed that CHIR-treated cells had downregulated *ID1* expression, whereas BMP4-treated

cells displayed marginally elevated expression. This finding is relevant because ID1 is one of the major downstream transcriptional targets of BMP signaling. It is also worth noting that BMP4 is directly upregulated by OVOL2, and that inhibition of BMP signaling by LDN-treated cells – along with WNT activation by CHIR-treated cells – downregulated *OVOL2* and *p63* expression (Fig. 4B). When we investigated eye developmental-related gene expression at 10 days of differentiation we found that CHIR-treated cells failed to express *PAX6*, *SIX3*, and *RAX* as major regulators of eye development (Fig. S3C–F).

3.6. Initiation of ocular surface ectodermal development by exposing cells to WNT inhibition and exogenous BMP4 during early stage development

Our initial experiments indicated that ocular surface ectoderm exhibited corneal epithelial commitment (i.e. the cells were p63+/PAX6+) in the paracentral zone of the immature pre-SEAM at 10 days of differentiation (Fig. 1C and D). To further probe the likely mechanisms at play, the three zones (i.e. central, paracentral, and peripheral) of the pre-SEAM colonies at 10 days of differentiation were isolated after which the gene expression levels in each zone were examined (Fig. 5A). This was done to test the hypothesis that WNT inhibition is involved in ocular surface ectodermal differentiation in the early stages of eye development. Major genes involved with WNT signaling inhibition were examined by qRT-PCR (Fig. S4B), and the results revealed that *SFRP2* and *DKK1* were substantially expressed amongst all WNT signaling antagonists. Notably, expression levels of *SFRP2*, encoding a negative regulator of canonical WNT signaling, exhibits similar expression patterns as *PAX6*. *SFRP1*, in contrast, revealed no correlation with *PAX6*. *DKK1*, a WNT signaling inhibitor, and *BMP4* were marginally more highly expressed in the paracentral zone among all zones (Fig. 5A), while *p63* expression correlated with that of *E-cadherin* as a surface ectoderm marker.

To investigate the chronology of *p63* and *PAX6* expression, cells from 0 to 14 days of differentiation were analyzed by qPCR. This revealed that *SFRP2* and *PAX6* were expressed as early as day 0, whereas *p63* expression was not seen until just before day 5 of development. Conversely, *LIN28A*, a marker of undifferentiated cells, decreased as differentiation progressed (Fig. S4A). SFPR2 and DKK1 secretion into culture medium, quantified by enzyme-linked immunosorbent assay (ELISA), revealed their presence at 3 days of differentiation (Fig. 5B and C). DKK1, in particular, was abundant in the culture medium at 3 days of differentiation. Neutralizing tests for SFRP2 and DKK1 conducted by blocking the functionality of endogenous, secreted SFRP2 was found to regulate and inhibit ocular surface ectodermal differentiation. Treatment of cells for the first 3 days of differentiation with a combination of SFRP2 and DKK1 antibodies was found to partially block autocrine SFRP2 and DKK1. At the same time, p63 expression was significantly reduced (Fig. 5D). The number of p63+/PAX6+ cells was considerably reduced in DKK1-treated cells and SFRP2 Ab and DKK1 Ab-treated cells, and moderately reduced in SFRP2 Ab-treated cells (Fig. 5E). Blocking secreted DKK1 by the use of a DKK1 antibody caused elevation of *AXIN2* and *LEF1* gene expression following activation of canonical WNT signaling (*WNT1* and *WNT3A*) (Fig. 5F). Fig. 6B shows a schematic based on published data (Fujimura, 2016; Giger and Houart, 2018; Li et al., 2013; Patthey et al., 2009) and the results presented herein, along
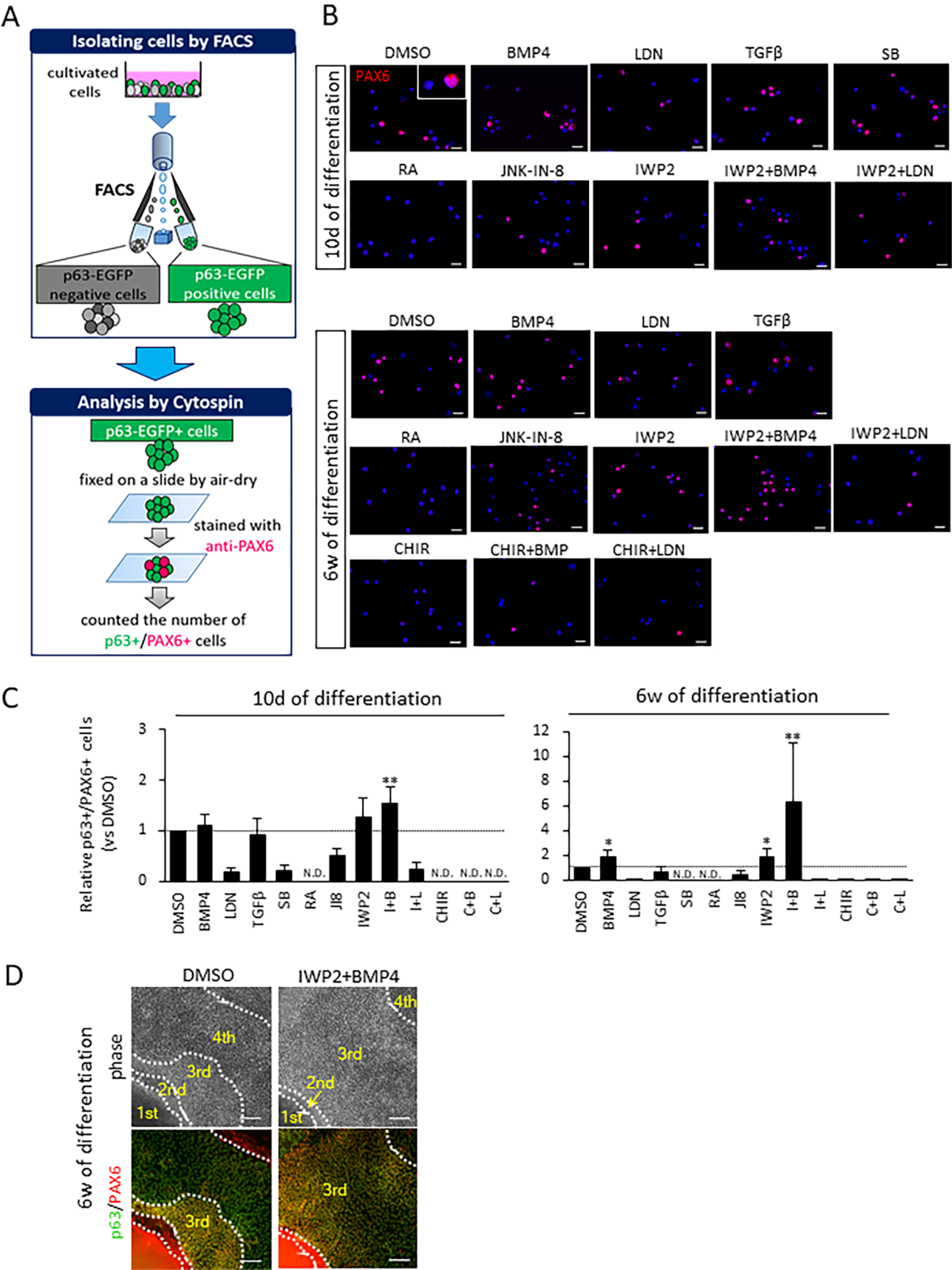
(caption on next page)

Fig. 3. p63/PAX6 differentiation efficiency. (A) Schematic of the experimental protocol for isolation of p63+ cells. The sorted cells were immunostained with PAX6 (red) followed by cytospin analysis and quantification of the ratio of p63+/PAX6+ in p63+ cells. (B) Immunostaining images of PAX6 positive cells in sorted p63-EGFP positive cells at 10 days and 6 weeks of differentiation. Nuclei, blue (scale bar, 20 μm). (C) Differentiation efficiency of p63+/PAX6+ cells. The number was calculated from the relative total cell number × relative EGFP number × relative number of p63+/PAX6+ positive cells. Data shown as the mean ± SD (n = five independent experiments). *p < 0.05, and **p < 0.01. N.D. Not Determined. A dashed line indicates a normalized value based on DMSO controls. (D) Immunostaining for ocular cells markers. Co-expression of p63 (green) and PAX6 (red) was detected in the SEAM at 6 weeks of differentiation. Nuclei, blue (scale bar, 100 μm).

with our interpretation of the information and its fit with mechanisms of eye development. Of note, is the idea of a differential "head vs trunk" mode of surface ectodermal differentiation and the emergence of the ocular surface ectoderm – and subsequently the ocular surface epithelium – via the head, with cell fate determined by the inhibition of canonical WNT signaling and BMP4.

4. Discussion

Ocular/head surface ectoderm development was studied using a p63-EGFP knock-in hiPSC reporter line, which allows us to specifically trace epithelial stem/progenitor cells. BMP4 and the WNT pathway have been fairly widely studied and are known to be instrumental in defining ectodermal-epithelial cell fate and in repressing neural fate (Aberdam et al., 2007; Cruciat and Niehrs, 2013; Groves and LaBonne, 2014; Metallo et al., 2008; Wilson and Hemmati-Brivanlou, 1995). With
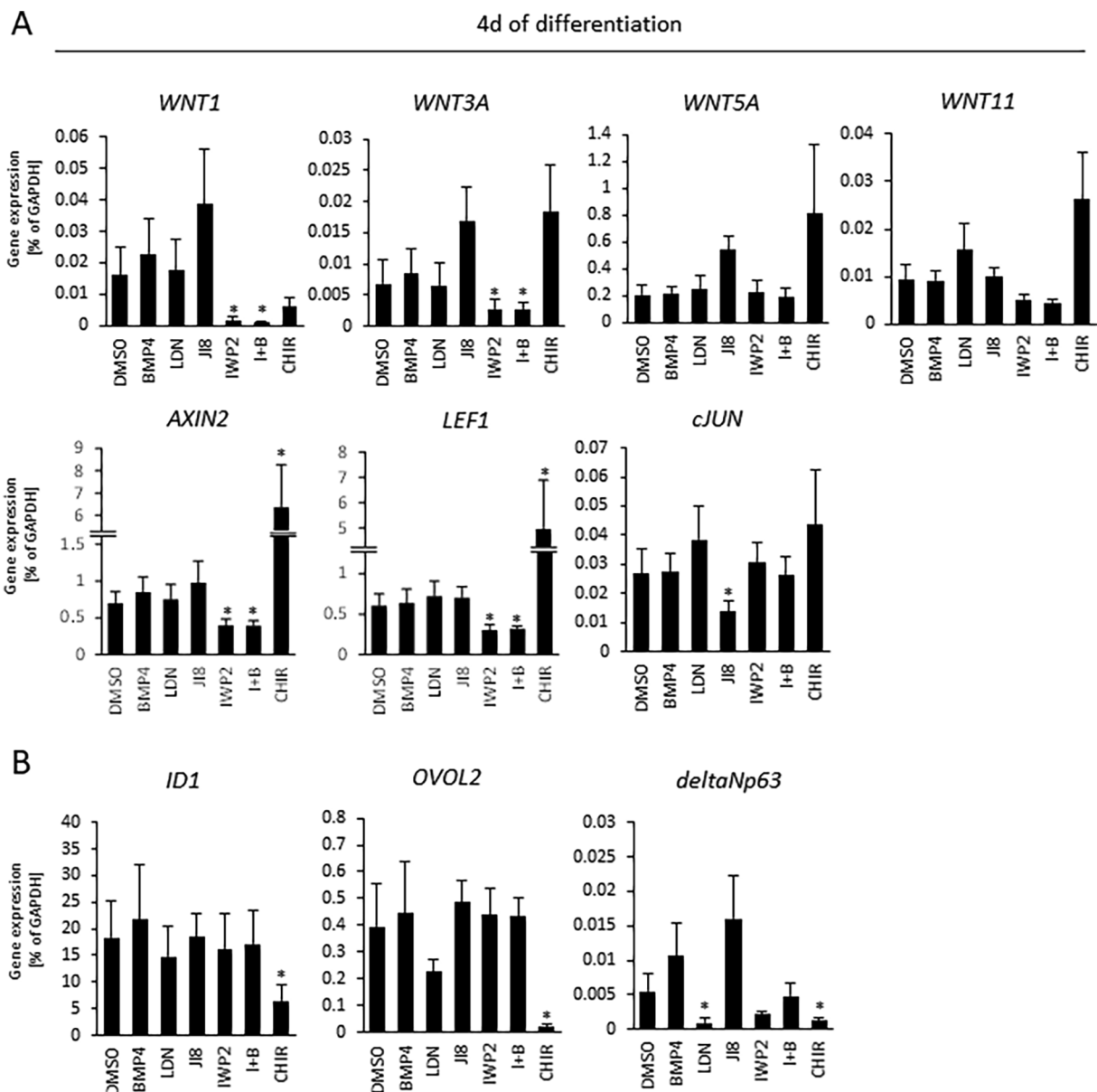

Fig. 4. Expression levels of WNT signaling and BMP4 signaling-related markers at 4 days of differentiation. (A) Quantitative gene expression of WNT ligands and downstream genes; WNT1, WNT3A, AXIN2, LEF1 as markers associated with the canonical pathway, and WNT5A, WNT11, cJUN as markers associated with the non-canonical pathway. (B) Quantitative gene expression of BMP4 related genes; ID1 is a major downstream transcriptional marker of BMP4, and OVOL2 and p63 are directly regulated by BMP4 expression. Data shown as the mean ± SD (n = five independent experiments). Asterisk represents statistical differences (*p < 0.05).
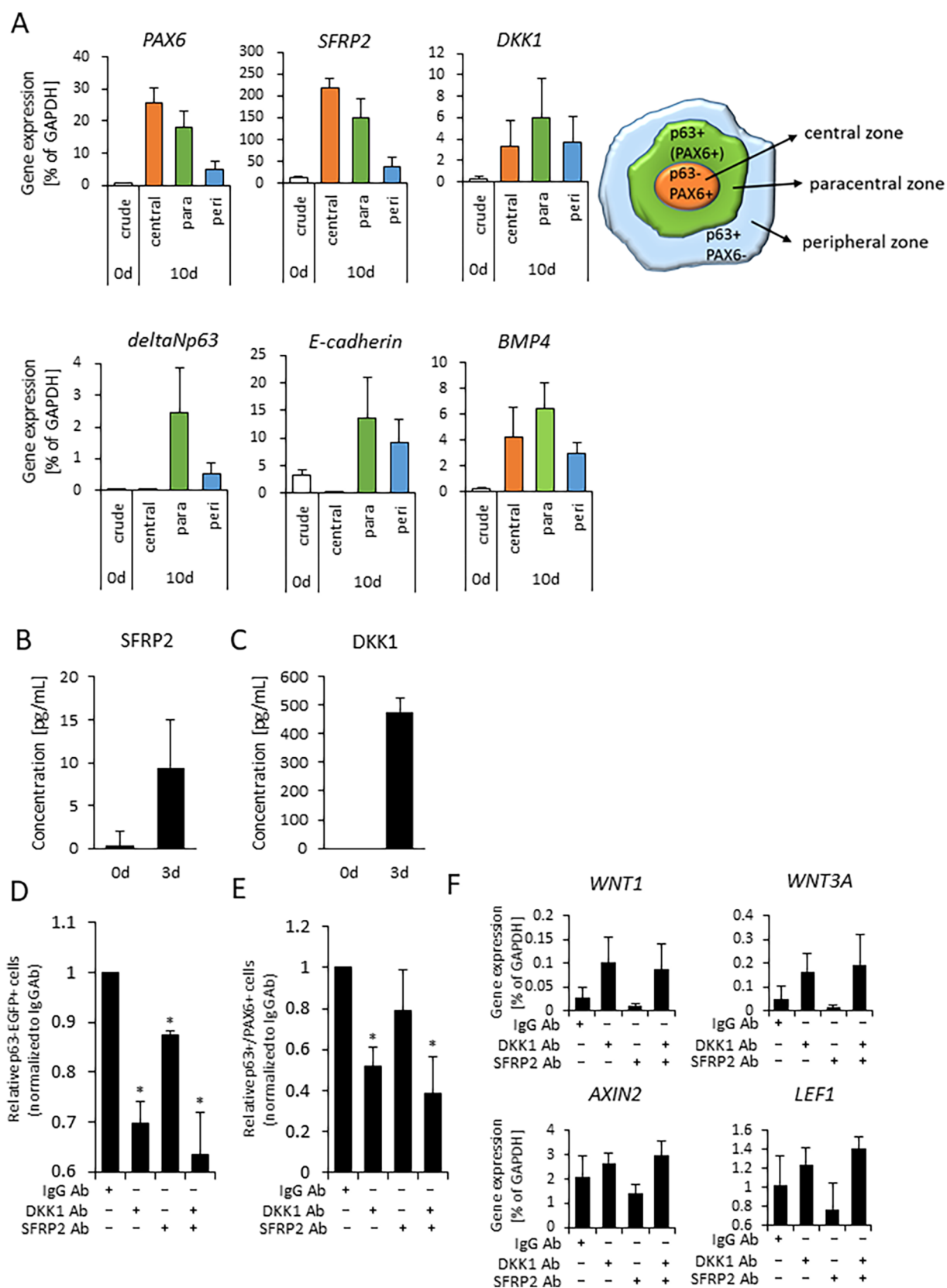
(caption on next page)

Fig. 5. SFRP2 and DKK1 secretion and expression during early differentiation. (A) Gene expression of central, paracentral (para), and peripheral (peri) zones of a pre-SEAM at 10 days of differentiation (3 to 5 colonies per sample for one experiment, n = five independent experiments). (B)(C) ELISA analysis for SFRP2 or DKK1 secretion in cell culture supernatants. The supernatant at day 0 was collected at the start of differentiation (i.e. after 10 days of hiPSC culture in StemFit), whereas the supernatants at day 3 were collected after 3 days of differentiation medium (DM) culture (independent experiments; n = four for day 0 and n = four for day 3). (D) Relative p63-EGFP positive cells population at 10 days of differentiation. The cells were neutralized by endogenously secreted SFRP2 and DKK1 using antibodies SFRP2 mAb 80.8.6, DKK1 pAb, or SFRP2 mAb + DKK1 pAb, which were added to the wells for 3 days. Mouse IgG2ακ and goat IgG (100 μg/ml) were used for internal controls (independent experiments; n = five for IgG, DKK1 pAb, and SFRP2 mAb + DKK pAb, n = four for SFRP2 mAb). Data shown as a normalized value based on DMSO controls. Asterisk represents statistical differences (*$p < 0.05$) (E) Differentiation efficiency of p63+/PAX6+ cells. The number was calculated from the relative total cell number × relative EGFP number × relative number of p63+/PAX6+ positive cells. Data shown as the mean ± SD (independent experiments; n = five for IgG, DKK1 pAb, and SFRP2 mAb + DKK pAb, n = four for SFRP2 mAb). Data shown as a normalized value based on DMSO controls. Asterisk represents statistical differences (*$p < 0.05$) (F) Quantitative gene expression of canonical WNT signaling; WNT1 and WNT3A, downstream targeting genes; AXIN2 and LEF1. Data shown as the mean ± SD (n = three independent experiments).

regards to the corneal epithelium, other groups have shown how corneal epithelial progenitors can be induced from iPSCs using BMP4, RA and, EGF (Kamarudin et al., 2018), or from hPSCs using IWP2, FGF and, SB431542 (Hongisto et al., 2017; Mikhailova et al., 2014). The latter was achieved, in part, because of the suppression of neuroectodermal commitment by the TGFβ signaling inhibitor, SB431542. These and similar studies allude to cell differentiation into corneal epithelial cells, but they are indicative rather than definitive and do not specifically delineate the ocular surface ectodermal cell fate and the differentiation processes involved. PAX6 single positive cells can differentiate into cells of the neuron, neural crest, or neural retina (Shaham et al., 2012), whereas p63 single positive cells can terminally differentiate into any type of stratified epithelial cells (e.g. corneal epithelium, skin epidermis, or oral mucosal cells) (Barbieri and Pietenpol, 2006; McKeon, 2004; Senoo et al., 2007). Thus, p63 co-stained with PAX6 is needed to prove that cells are ocular surface ectoderm, and the results presented here utilize our previously generated p63-EGFP knock-in hiPS cells (Kobayashi et al., 2017) to do this and indicate that p63+/PAX6+ cells of an ocular surface ectodermal phenotype are present in the very early stages of eye development. We also show that autocrine BMP4 signaling and WNT inhibition during hiPSC differentiation *in vitro* play fundamental roles in the development of ocular surface ectodermal and epithelial cell lineages.

In order to interrogate the effect of secreted signals during early differentiation cells were treated with enhancing and/or inhibiting signals (e.g. WNT signaling, BMP4, TGFβ and additional RA) for the first 4 days of differentiation, and this clearly revealed that the morphology of the pre-SEAM and SEAM was distinctively different with various p63 expression patterns. It was notable that the immature pre-SEAM structures that had formed at 10 days of differentiation were not able to recover a SEAM-like morphology, even when cultivated for 6 weeks of differentiation (Fig. 2A and B). This suggests that cell fate *in situ* is likely determined early in development via WNT inhibition and BMP4 signaling. Findings from IWP2 and BMP4 treated cells revealed that within the first 4 days of differentiation is the critical period that seals the fate of the differentiating cells, and that the period immediately after this (i.e. 4 to 7 days) has no influence on the pattern of differentiation (Fig. S1A–F).

In mouse embryos, the epiblast at embryonic day (E) 5.5 has pluripotency. Gastrulation begins at E6.5 and surface ectoderm and neural ectoderm are committed by E7.5 (Li et al., 2013). Ordinarily, developing mouse eyes are not often studied before the initiation of presumptive lens invagination at E9.5, but here we conducted immunostaining at E8.5, which identifies p63+/Pax6+ cells localized within an area in which cells are believed to commit to become ocular surface epithelium (Fig. 1E) (Collomb et al., 2013). Based on the expression patterns of PAX6 and p63, our findings imply that hiPSCs that differentiate into ocular surface ectoderm correlate to the E8.5–E9.5 mouse eye at 10–14 days of differentiation (Hayashi et al., 2016).

Previous studies have shown that the loss of PAX6 in developing corneal epithelial cells results in a conversion to epidermal development (Collomb et al., 2013; Ouyang et al., 2014). Here, we show that cells treated with RA and CHIR express p63, but not PAX6. Moreover,

analysis of the HOX gene expression pattern (Okubo et al., 2018) suggests that p63+ CHIR-treated cells are destined towards trunk epithelial patterning (e.g. feet and legs), whereas the fate of p63+ RA-treated cells are likely that of the facial epithelia, such as the eyelids, cheek and neck tissue (Fig. S2). We thus contend that p63 in ocular surface ectoderm expresses much earlier than p63 in epidermis. Although RA is a widely accepted factor for the induction of epidermis via ectoderm development (Metallo et al., 2008), treatment with RA early in the expansion of hiPSCs into a SEAM does not result in the development of the ocular surface ectoderm and the corneal epithelium due to suppression of PAX6.

Other investigators have shown that SFRPs and/or DKK1 coordinately control forebrain development (including the development of ocular precursors) (Lewis et al., 2008; Mukhopadhyay et al., 2001) and that a DKK1 ± haploinsufficiency leads to developmental eye disorders (Giger and Houart, 2018; Lieven and Ruther, 2011). SFRP2, moreover, is an essential downstream target of PAX6, and plays a significant role in the generation of presumptive corneal epithelial cells in the ocular surface ectoderm during eye development (Shaham et al., 2012). It is only expressed during early embryonic development (Chen et al., 2004), regulated by PAX6 (Machon et al., 2010). Our data shows that the central zone in the pre-SEAMs abundantly expresses *SFRP2*, which is followed by *PAX6* expression. *DKK1*, on the other hand, is expressed throughout all zones, but is especially prominent in the paracentral zone (Fig. 5A). Thus, we showed the specification of the ocular surface ectoderm is precisely controlled by WNT/β-catenin inhibition through SFRP2 and DKK1 along with exposure to BMP4 signaling. It is also known that the BMP4 signaling dose determines the direction for neural ectoderm or non-neural ectoderm via WNT signaling mediation (Fujimura, 2016; Leung et al., 2016; Patthey et al., 2009; Stern, 2005). Simultaneously, BMP4 initiates p63 and E-cadherin expression in the paracentral and peripheral zones of the pre-SEAM, thus p63+/E-cadherin+/PAX6+ cells are ocular surface ectoderm and the paracentral zone is destined to become SEAM zone 3 representing the ocular surface ectoderm. Of note, our investigations found that inhibition of JNK (i.e. non-canonical WNT signaling) increased p63 expression, but not the amount of corneal epithelial cells. This implies that canonical WNT inhibition is predominantly involved in early corneal epithelial development. Based on our evidence, a crucial event in the development of the ocular surface ectoderm is considered to be the secretion of sufficient SFRP2 via PAX6 expression, as well as the presence of enough DKK1 for WNT signaling inhibition. Indeed, we found no significant gene expression changes among other major WNT antagonists (Fig. S4B), and thus conclude that SFRP2 and DKK1-mediated WNT inhibition are likely instrumental in the formation of the ocular surface ectoderm. Experiments in which SFRP2 and DKK1 were mildly blocked by specific antibodies confirmed upregulated *WNT1* and *WNT3A* by DKK1 neutralization (Fig. 5F), however, at the amounts used the blocking was not able to influence the function of WNT inhibition.

Here, we offer a schematic representation of *in vivo* and *in vitro* eye development in an E8.5 mouse embryo and in hiPSCs after 10 days of differentiation, respectively. This denotes how WNT inhibition and
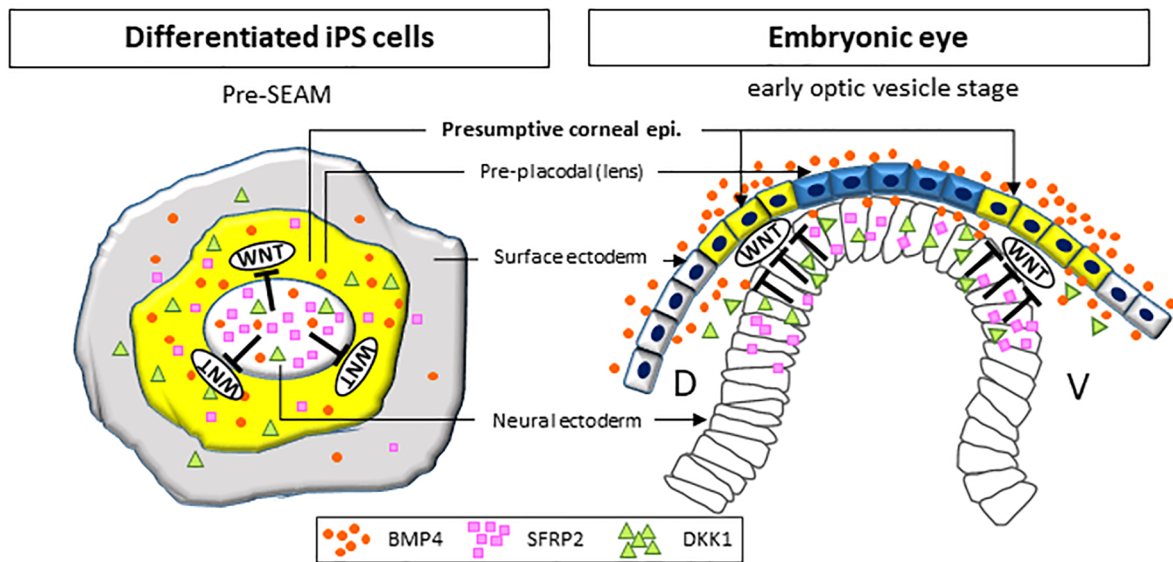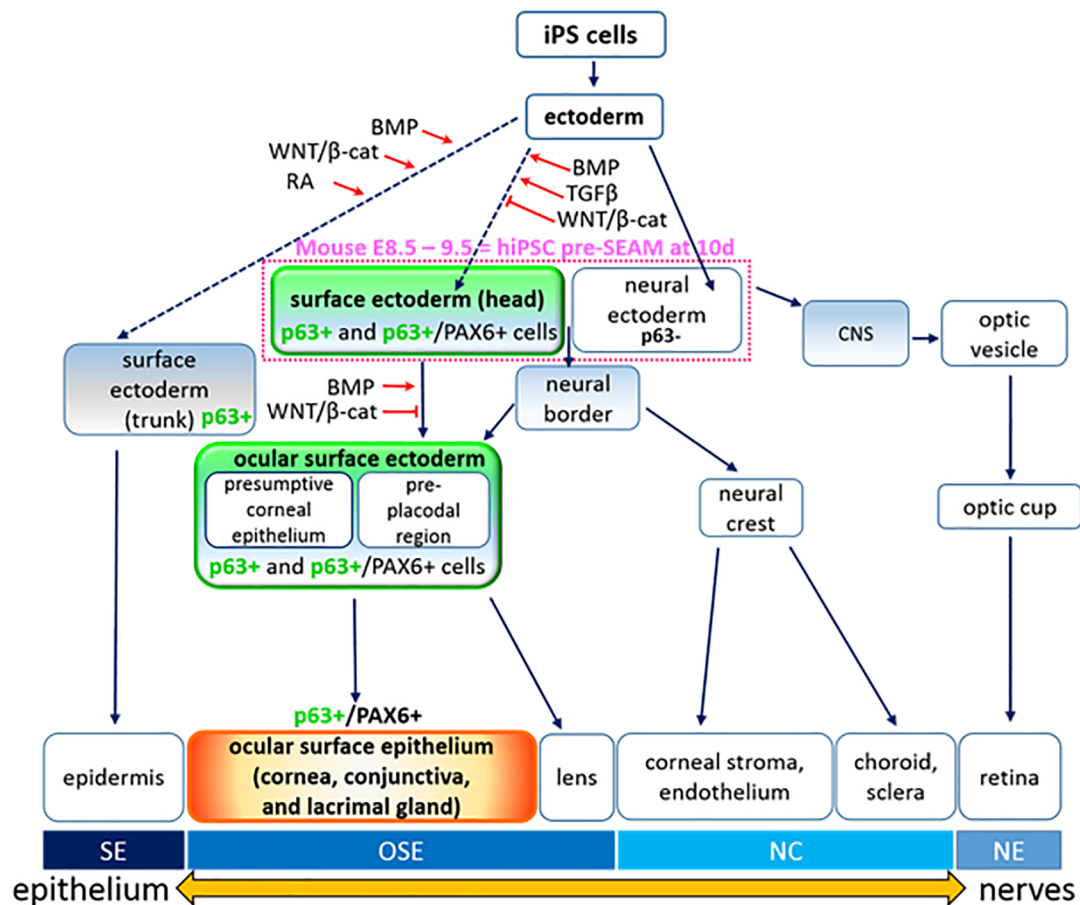
Fig. 6. Development of ocular surface ectodermal cell lineages from human induced pluripotent stem cells. (A) Schematic representation of *in vivo* and *in vitro* of eye development with BMP and WNT signaling pathways. The upper diagram shows an early optic vesicle stage at mouse embryonic stage E8.5, whereas the bottom diagram shows a pre-SEAM structure at 10 days of hiPSC differentiation. Gene expression patterns and cell lineages in the central, paracentral and peripheral zones in a pre-SEAM correlate to mouse E8.5 are indicated by black arrows based on the results of Fig. 5A. D, dorsal; V, ventral. (B) Schematic image of eye related organ development. The dotted lines indicate our findings that WNT inhibition and BMP signaling trigger corneal epithelial commitment. The red arrows indicate the newly proposed signaling pathway.

BMP4 signaling are involved in the development of the ocular surface epithelium. The model proposes that the optic vesicle (i.e. neural ectoderm) contacts physically with the head surface ectoderm, and that this is the hallmark event of head surface ectoderm development that leads to differentiation of the presumptive corneal epithelium and preplacodal region by the various inductive signals (Fig. 6A).

5. Conclusions

Our findings demonstrated new aspects about the process of human eye development by focusing on ocular surface ectodermal cell fate determination, based upon data acquired from a hiPSC-derived SEAM model which mimics human eye development. We discovered that SFRP2 and DKK1 act as putative antagonists of canonical WNT signaling and are both expressed in neural ectoderm in differentiating hiPSCs. Simultaneously, BMP4 initiates non-neural ectodermal differentiation into a corneal epithelial lineage. We also found that combined treatment of hiPSCs with exogenous BMP4 aligned to WNT inhibition for an initial period of 4 days of differentiation significantly increased the ocular surface ectodermal cell population and induced a corneal epithelial fate. Our results reveal that ocular surface ectodermal lineage is controlled by endogenous BMP4 signaling and the inhibition of WNT signaling at the very earliest stages of hiPSC differentiation (Fig. 6B). Therefore, we conclude that PAX6 (neural ectodermal marker) initially determines eye position during gastrulation, and thereafter SFRP2 and DKK1 mediate WNT signaling inhibition and promote the development of the ocular surface ectoderm (i.e. p63 + /PAX6 + cells). At the same time, BMP4 is secreted to drive epithelial differentiation as a critical part of the eye's development.

CRediT authorship contribution statement

Yuki Kobayashi: Conceptualization, Validation, Formal analysis, Investigation, Writing - original draft, Writing - review & editing, Visualization. **Ryuhei Hayashi:** Conceptualization, Formal analysis, Writing - review & editing, Supervision, Funding acquisition. **Shun Shibata:** Conceptualization, Writing - review & editing. **Andrew J. Quantock:** Writing - review & editing, Supervision, Funding acquisition. **Kohji Nishida:** Supervision, Funding acquisition.

Declaration of Competing Interest

The authors declare that they have no known competing financial interests or personal relationships that could have appeared to influence the work reported in this paper.

Acknowledgements

Author contributions

Y.K., R.H., S.S., and K.N. designed the research. Y.K. and R.H. designed and analyzed the data. Y.K. performed the experiments and acquired the data. Y.K., R.H., and A.J.Q. interpreted the data and wrote the manuscript. R.H., A.J.Q., and K.N. obtained financial support.

Appendix A. Supplementary data

Supplementary data to this article can be found online at https://doi.org/10.1016/j.scr.2020.101868.

References

Aberdam, D., Gambaro, K., Rostagno, P., Aberdam, E., de la Forest Divonne, S., Rouleau, M., 2007. Key role of p63 in BMP-4-induced epidermal commitment of embryonic stem cells. Cell Cycle 6, 291–294. https://doi.org/10.4161/cc.6.3.3800.

Barbieri, C.E., Pietenpol, J.A., 2006. p63 and epithelial biology. Exp. Cell Res. 312, 695–706. https://doi.org/10.1016/j.yexcr.2005.11.028.

Chen, Y., Stump, R.J., Lovicu, F.J., McAvoy, J.W., 2004. Expression of Frizzleds and secreted frizzled-related proteins (Sfrps) during mammalian lens development. Int. J. Dev. Biol. 48, 867–877. https://doi.org/10.1387/ijdb.041882yc.

Collomb, E., Yang, Y., Foriel, S., Cadau, S., Pearton, D.J., Dhouailly, D., 2013. The corneal epithelium and lens develop independently from a common pool of precursors. Dev. Dyn. 242, 401–413. https://doi.org/10.1002/dvdy.23925.

Cruciat, C., Niehrs, C., 2013. Secreted and transmembrane Wnt inhibitors and activators. Cold Spring Harb. Perspect. Biol. 1–26.

Fujimura, N., 2016. WNT/beta-catenin signaling in vertebrate eye development. Front. Cell Dev. Biol. 4, 138. https://doi.org/10.3389/fcell.2016.00138.

Giger, F.A., Houart, C., 2018. The birth of the eye vesicle: when fate decision equals morphogenesis. Front. Neurosci. 12, 87. https://doi.org/10.3389/fnins.2018.00087.

Groves, A.K., LaBonne, C., 2014. Setting appropriate boundaries: fate, patterning and competence at the neural plate border. Dev. Biol. 389, 2–12. https://doi.org/10.1016/j.ydbio.2013.11.027.

Hayashi, R., Ishikawa, Y., Katori, R., Sasamoto, Y., Taniwaki, Y., Takayanagi, H., Tsujikawa, M., Sekiguchi, K., Quantock, A.J., Nishida, K., 2017. Coordinated generation of multiple ocular-like cell lineages and fabrication of functional corneal epithelial cell sheets from human iPS cells. Nat. Protoc. 12, 683–696. https://doi.org/10.1038/nprot.2017.007.

Hayashi, R., Ishikawa, Y., Sasamoto, Y., Katori, R., Nomura, N., Ichikawa, T., Araki, S., Soma, T., Kawasaki, S., Sekiguchi, K., Quantock, A.J., Tsujikawa, M., Nishida, K., 2016. Co-ordinated ocular development from human iPS cells and recovery of corneal function. Nature 531, 376–380. https://doi.org/10.1038/nature17000.

Hongisto, H., Ilmarinen, T., Vattulainen, M., Mikhailova, A., Skottman, H., 2017. Xeno- and feeder-free differentiation of human pluripotent stem cells to two distinct ocular epithelial cell types using simple modifications of one method. Stem Cell Res. Ther. https://doi.org/10.1186/s13287-017-0738-4.

Kamarudin, T.A., Bojic, S., Collin, J., Yu, M., Alharthi, S., Buck, H., Shortt, A., Armstrong, L., Figueiredo, F.C., Lako, M., 2018. Differences in the activity of endogenous bone morphogenetic protein signaling impact on the ability of induced pluripotent stem cells to differentiate to corneal epithelial-like cells. Stem Cells. https://doi.org/10.1002/stem.2750.

Kobayashi, Y., Hayashi, R., Quantock, A.J., Nishida, K., 2017. Generation of a TALEN-mediated, p63 knock-in in human induced pluripotent stem cells. Stem Cell Res. 25, 256–265. https://doi.org/10.1016/j.scr.2017.10.015.

Leung, A.W., Leung, A.W., Murdoch, B., Salem, A.F., Prasad, M.S., Gomez, G.A., García-Castro, M.I., 2016. WNT/β-catenin signaling mediates human neural crest induction via a pre-neural border intermediate. Development 143, 398–410. https://doi.org/10.1242/dev.130849.

Lewis, S.L., Khoo, P.L., De Young, R.A., Steiner, K., Wilcock, C., Mukhopadhyay, M., Westphal, H., Jamieson, R.V., Robb, L., Tam, P.P., 2008. Dkk1 and Wnt3 interact to control head morphogenesis in the mouse. Development 135, 1791–1801. https://doi.org/10.1242/dev.018853.

Li, L., Liu, C., Biechele, S., Zhu, Q., Song, L., Lanner, F., Jing, N., Rossant, J., 2013. Location of transient ectodermal progenitor potential in mouse development. Development 140, 4533–4543. https://doi.org/10.1242/dev.092866.

Lieven, O., Ruther, U., 2011. The Dkk1 dose is critical for eye development. Dev. Biol. 355, 124–137. https://doi.org/10.1016/j.ydbio.2011.04.023.

Machon, O., Kreslova, J., Ruzickova, J., Vacik, T., Klimova, L., Fujimura, N., Lachova, J., Kozmik, Z., 2010. Lens morphogenesis is dependent on Pax6-mediated inhibition of the canonical Wnt/beta-catenin signaling in the lens surface ectoderm. Genesis 48, 86–95. https://doi.org/10.1002/dvg.20583.

Matt, N., Dupe, V., Garnier, J.M., Dennefeld, C., Chambon, P., Mark, M., Ghyselinck, N.B., 2005. Retinoic acid-dependent eye morphogenesis is orchestrated by neural crest cells. Development 132, 4789–4800. https://doi.org/10.1242/dev.02031.

McKeon, F., 2004. p63 and the epithelial stem cell: More than status quo? Genes Dev. https://doi.org/10.1101/gad.1190504.

Melino, G., Memmi, E.M., Pelicci, P.G., Bernassola, F., 2015. Maintaining epithelial stemness with p63. Sci. Signal 8, re9. https://doi.org/10.1126/scisignal.aaa1033.

Metallo, C.M., Ji, L., de Pablo, J.J., Palecek, S.P., 2008. Retinoic acid and bone morphogenetic protein signaling synergize to efficiently direct epithelial differentiation of human embryonic stem cells. Stem Cells 26, 372–380. https://doi.org/10.1634/stemcells.2007-0501.

Mikhailova, A., Ilmarinen, T., Uusitalo, H., Skottman, H., 2014. Small-molecule induction promotes corneal epithelial cell differentiation from human induced pluripotent stem cells. Stem Cell Rep. 2, 219–231. https://doi.org/10.1016/j.stemcr.2013.12.014.

Mukhopadhyay, M., Shtrom, S., Rodriguez-Esteban, C., Chen, L., Tsukui, T., Gomer, L., Dorward, D.W., Glinka, A., Grinberg, A., Huang, S.P., Niehrs, C., Izpisua Belmonte, J.C., Westphal, H., 2001. Dickkopf1 is required for embryonic head induction and limb morphogenesis in the mouse. Dev. Cell 1, 423–434.

Nakagawa, M., Taniguchi, Y., Senda, S., Takizawa, N., Ichisaka, T., Asano, K., Morizane,

A., Doi, D., Takahashi, J., Nishizawa, M., Yoshida, Y., Toyoda, T., Osafune, K., Sekiguchi, K., Yamanaka, S., 2014. A novel efficient feeder-free culture system for the derivation of human induced pluripotent stem cells. Sci. Rep. 4, 3594. https://doi.org/10.1038/srep03594.

Okubo, T., Hayashi, R., Shibata, S., Kudo, Y., Honma, Y., Nishida, K., 2018. Use of homeobox gene expression patterns to determine anatomical regions of origin for body surface tissues derived from adult mice. J. Tissue Eng. Regen. Med. 12, 1412–1419. https://doi.org/10.1002/term.2673.

Ouyang, H., Xue, Y., Lin, Y., Zhang, X., Xi, L., Patel, S., Cai, H., Luo, J., Zhang, Meixia, Zhang, Ming, Yang, Y., Li, G., Li, H., Jiang, W., Yeh, E., Lin, J., Pei, M., Zhu, J., Cao, G., Zhang, L., Yu, B., Chen, S., Fu, X.D., Liu, Y., Zhang, K., 2014. WNT7A and PAX6 define corneal epithelium homeostasis and pathogenesis. Nature 511, 358–361. https://doi.org/10.1038/nature13465.

Patthey, C., Edlund, T., Gunhaga, L., 2009. Wnt-regulated temporal control of BMP exposure directs the choice between neural plate border and epidermal fate. Development 136, 73–83. https://doi.org/10.1242/dev.025890.

Senoo, M., Pinto, F., Crum, C.P., McKeon, F., 2007. p63 is essential for the proliferative potential of stem cells in stratified epithelia. Cell. https://doi.org/10.1016/j.cell.2007.02.045.

Shaham, O., Menuchin, Y., Farhy, C., Ashery-Padan, R., 2012. Pax6: a multi-level regulator of ocular development. Prog. Retin. Eye Res. 31, 351–376. https://doi.org/10.1016/j.preteyeres.2012.04.002.

Shibata, S., Hayashi, R., Okubo, T., Kudo, Y., Katayama, T., Ishikawa, Y., Toga, J., Yagi, E., Honma, Y., Quantock, A.J., Sekiguchi, K., Nishida, K., 2018. Selective laminin-directed differentiation of human induced pluripotent stem cells into distinct ocular lineages. Cell Rep. 25, 1668–1679 e5. https://doi.org/10.1016/j.celrep.2018.10.032.

Soares, E., Zhou, H., 2018. Master regulatory role of p63 in epidermal development and disease. Cell Mol. Life Sci. 75, 1179–1190. https://doi.org/10.1007/s00018-017-2701-z.

Stern, C.D., 2005. Neural induction: old problem, new findings, yet more questions. Development 132, 2007–2021. https://doi.org/10.1242/dev.01794.

Sugiyama, Y., Shelley, E.J., Wen, L., Stump, R.J., Shimono, A., Lovicu, F.J., McAvoy, J.W., 2013. Sfrp1 and Sfrp2 are not involved in Wnt/beta-catenin signal silencing during lens induction but are required for maintenance of Wnt/beta-catenin signaling in lens epithelial cells. Dev. Biol. 384, 181–193. https://doi.org/10.1016/j.ydbio.2013.10.008.

Wilson, P.A., Hemmati-Brivanlou, A., 1995. Induction of epidermis and inhibition of neural fate by Bmp-4. Nature. https://doi.org/10.1038/376331a0.

Yoh, K., Prywes, R., 2015. Pathway regulation of p63, a director of epithelial cell fate. Front. Endocrinol. 6, 51. https://doi.org/10.3389/fendo.2015.00051.